J. Electroanal. Chem., 332 (1992) 1–31
Elsevier Sequoia S.A., Lausanne
JEC 02021

Analysis of experiments on the calorimetry of LiOD–D_2O electrochemical cells

R.H. Wilson, J.W. Bray, P.G. Kosky, H.B. Vakil and F.G. Will *
GE Corporate Research and Development, P.O. Box 8, Schenectady, NY 12301 (USA)
(Received 24 June 1991; in revised form 16 December 1991)

Abstract

In this paper we present a detailed analysis of calorimetry with heavy-water electrolytic cells, especially of the type described by Pons, Fleischmann and co-workers in recent publications. We also summarize our own experiments, which involve calorimetry of electrolytic cells of various designs. None of our experiments has yielded any excess heat or radiation products within the detection limits. We evaluate the data and methods of Pons, Fleischmann and co-workers and, where sufficient data are available, conclude that they overestimate significantly the excess heat. This is in part because in their calibration they did not include calculation of the change in input electrochemical power to the cell resulting from the calibration heater power. An additional significant overestimate of excess energy occurs when the calibration is made at cell temperatures above about 60°C, owing to the increased evaporation of heavy water during the calibration. Furthermore, we find unexplainable inconsistencies in the data on light-water controls, as reported by Pons and Fleischmann. While our analysis shows their claims of continuous excess heat generation to be overstated significantly, we cannot prove that no excess heat has been generated in any experiments.

INTRODUCTION

In this paper we present a detailed analysis of the type of calorimetry described in recent publications by Pons, Fleischmann and co-workers (PF) [1–3]. These publications provide more details about their measurement of excess heat, which they ascribed to "nuclear fusion" in their original publications [4,5]. We also discuss briefly our own experiments, which involve calorimetry of electrochemical cells of various designs, using palladium as the cathode and LiOD in D_2O as the electrolyte. None of our experiments has yielded any excess heat.

* Present address: Dept. of Chemical Engineering, University of Utah, Salt Lake City, UT 84112, USA.

We evaluate the data and methods of PF and conclude that they overestimate the excess heat. This is because they do not include the change in power and D_2O evaporation in the electrochemical cell in their calibration calculation. For those results where sufficient data are available, we show that the overestimate using their "approximate" method is significant. Furthermore, we show where the equivalent error can be made in their regression analysis and argue that this is how they obtain agreement between the excess heats calculated by the two methods described in their publications. If the correct calibration procedures were used for all their results, the strong correlation between excess heat and current density would probably disappear. We do not prove that no excess heat has been generated in any PF experiments; for example, the "burst" data that they present is not greatly reduced by the corrections that we describe. If excess energy is being generated, however, it is important that the factors that control its release be investigated. It is possible that the strong dependence on current density that PF report may misdirect that investigation.

The control experiments reported by PF also pose a dilemma. Using their approximate method to calculate excess heats, they find no excess heat within a few milliwatts. If, however, they used the procedures that they describe for determining excess heat, they should have obtained significant positive values as a result of neglecting the effects described above. The results that they report are inconsistent with the procedures that they describe.

We believe that the PF-type cell is capable of satisfactory calorimetry when properly calibrated. However, we believe that the calibration procedures that they use, the consistency of their results, and the precision that they claim are open to question. These issues are discussed in the following sections.

CALORIMETRY IN AN OPEN SYSTEM OF THE PONS–FLEISCHMANN TYPE

An open system from which vapor is allowed to escape adds a number of terms to the usual energy balance equations used in calorimetry. A correct analysis of such a system, included in Appendix A, shows that several terms are not properly accounted for in the PF discussion [1–3]; fortunately, these do not lead to significant errors in their calculation of excess heat.

Other potential sources of error in their experimental procedures have been suggested. One of these, inadequate mixing within the cell, leading to thermal gradients, does not appear to be a problem [3]. Another, the possible recombination of oxygen and deuterium within the cell, is apparently eliminated by careful accounting for the amount of heavy water required to replace the water lost by electrolysis. This measurement is complicated, however, by the uncertainty in the amount of heavy-water vapor that leaves the cell together with the electrolyzed oxygen and deuterium gases. This is not believed to be an issue in the PF results. A third potential error is in their heat loss calibration procedure, which is discussed in the following paragraphs.

Measurement of excess heat depends on the ability to calibrate accurately the rate of heat loss from the cell as a function of the cell and bath temperature. The calibration of the system used by PF is complicated by several factors. One is the change in electrolyte level caused by the electrolysis of water during electrochemical operation. Another is that radiation plays an important role in the heat loss, making the loss non-linear in the temperature difference between the cell and the bath in which the cell is immersed. These factors are evaluated in Appendix B and compared with experimental results using a cell like that used by PF. The heat loss is shown to be about half radiation and half conduction, with the ratio changing slightly with the electrolyte level.

Proper calibration of the heat loss involves measuring the cell temperature versus net power into the cell for a range of cell temperatures, bath temperatures and electrolyte levels. To avoid this complication, PF have chosen a single bath temperature and a differential calibration procedure. This procedure, while adding to experimental error, is acceptable if performed properly, as described in the next section.

Wagner et al. [6] have recently discussed the problems associated with this type of open cell calorimetry. One problem, the change in cell conditions with electrolyte level, is well recognized by PF. They interpolate their calibration to a single moment in time in their approximate method, which is the method recommended in ref. 6. In their regression analysis, PF include this time dependence as a parameter in their analysis.

A second problem reviewed by Wagner et al. is the change in cell impedance associated with the calibration procedure. This effect is discussed in the next section and evaluated for PF data in the subsequent analysis section.

A third problem, not recognized by Wagner et al., is the effect of vapor loss during calibration. This is also discussed and quantified in the following sections.

Finally, Wagner et al. describe the need for a "thermally controlled environment" in this type of calorimetry. Their measurements of heat loss were erratic when their cell was immersed in a water bath with no insulating layer. The erratic behavior, however, was the result of heat loss rates of more than 50 mW K^{-1} cm^{-2} which led to temperature gradients in the bath surrounding the cell and in the cell itself. Their other measurements had heat loss rates of 17 mW K^{-1} cm^{-2} and gave reproducible results. In the PF experiments the heat loss rate was about 1 mW K^{-1} cm^{-2} so that these gradients were not important in their work.

With the precautions discussed here, open-cell calorimetry of the PF type is capable of giving satisfactory results with 5–10% accuracy. Much of this uncertainty is introduced by the differential calibration and the correction terms that PF neglect. These are discussed in the next section.

CELL CALIBRATION BY DIFFERENTIAL POWER INPUT

One calibration procedure used by PF can readily be understood and reproduced. With this procedure they obtain what they refer to as "approximate" excess

energies. A second calibration procedure, which uses the same experimental data in multiparameter regression analysis, is very complicated and very difficult to follow in detail. This procedure is used to obtain what they refer to as "exact" excess energies. Both depend on an experimental procedure that introduces a known incremental power into the cell during operation. The associated temperature change introduces changes in the cell operation that are not taken into account in their approximate procedures. As is shown in the next section, these effects reduce the calculated excess energy significantly when they are included in the approximate procedure. Since the excess energy that they obtain from their regression analysis agrees so closely with the values that they obtain from their incorrect approximate procedure, it seems clear that a similar error must occur in their regression analysis. In this section the effects that they neglect in their approximate calculation are discussed in detail. In addition, a possible error in their exact calculation that is mathematically equivalent to the error in their approximate calculation is described.

Effect of power into the calibration heater

As shown in Appendix B, a cell like that of PF loses about one half of its heat by radiation. This makes the heat loss non-linear in temperature and complicates the calibration procedure by introducing a second unknown experimental parameter. Furthermore, in their open cell the electrolyte level is changing so that the heat loss parameters are continually changing. They choose to avoid these complications by doing differential calibration during operation and by using a single heat loss parameter k'_R, treating all heat loss as radiative. They argue that this underestimates excess energy. This parameter is defined by

$$Q = k_R(T_c^4 - T_b^4) + k_c(T_c - T_b) = k'_R(T_c^4 - T_b^4) \tag{1}$$

where Q is the heat loss rate from the cell when the cell is at temperature T_c and the bath at T_b. The parameters k_R and k_c are the correct heat loss parameters whose values are discussed in Appendix B.

To determine the value of k'_R, PF start with the cell in an initial quasi-steady state, add a small amount of power P_h to the cell, and wait until a new quasi-steady state is established; they then turn off the incremental power and wait until a final quasi-steady state is established. By interpolating their measurements between the initial and final states to compare with the measurements made with the incremental power on, they avoid satisfactorily the effect of electrolyte level change and obtain a value for k'_R.

To obtain the correct value for k'_R, all changes in cell operation induced by the calibration heater must be taken into account. These are discussed in detail in Appendix A; those that are quantitatively important are included here.

The interpolated heat loss rate Q_1 without the incremental power from the heater is given by

$$Q_1 = I_1(E_1 - E^c_{tn_1} - B_1) + Q_{f_1} \tag{2}$$

where I_1 is the cell current, E_1 is the cell potential, $I_1 E^c_{tn_1}$ is the rate of enthalpy removal from the cell by the electrolysis of D_2O, $I_1 B_1$ is the rate of enthalpy removal from the cell by the evaporation of the D_2O vapor carried out of the cell with the D_2 and O_2 gases produced by electrolysis and Q_{f_1} is any excess energy being generated in the cell by unknown processes. These values are, of course, interpolated between the initial and final states without incremental power to correspond to the point in time when the values with the heater on are determined.

Similarly, the heat loss rate Q_2 at the same time when the heater power P_h is on is

$$Q_2 = P_h + I_2\left(E_2 - E^c_{tn_2} - B_2\right) + Q_{f_2} \tag{3}$$

Using eqns. (1)–(3) we obtain

$$k'_R = \frac{P_h + I\left[\left(E_2 - E_1\right) - \left(E^c_{tn_2} - E^c_{tn_1}\right) - \left(B_2 - B_1\right)\right] + \left(Q_{f_2} - Q_{f_1}\right)}{T^4_{c_2} - T^4_{c_1}} \tag{4}$$

when constant current is assumed. Values of E are measured and are seen to decrease with increasing temperature, thereby making the calculated value of k'_R smaller. As will be seen in the next section, this effect can be large. The temperature dependence of E^c_{tn} is known and is small. The value of B can be calculated from

$$B = \frac{3}{4F}\frac{P}{P^* - P}L \tag{5}$$

where F is the Faraday constant, P is the vapor pressure of D_2O over the electrolyte, P^* is atmospheric pressure and L is the latent heat of D_2O evaporation at cell temperature. B increases with increasing temperature, and its change also decreases the calculated value of k'_R. Its effect becomes important at cell temperatures above 60°C. Measuring Q_f is, of course, the objective of the experiments; so its temperature dependence is not known. It is worth noting, however, that it could affect the calibration. All these temperature-dependent effects could be avoided if the cell temperature during calibration were held constant by reducing the bath temperature.

The effect of the change in E has been discussed by Wagner et al. [6] and they showed its importance in their experimental results. They did not discuss the effect of changes in B.

Critique of the Pons–Fleischmann analysis

In their "approximate" calculations of excess energy, PF neglect all the terms in eqn. (4) except P_h. In ref. 2 this amounts to assuming that Q in their eqn. (2) is the same as Q in eqn. (1). (There is a typographical error in eqn. 4 of ref. 2 that shows Q instead of ΔQ.) In ref. 1 the error is equating Q in eqn. (3) with Q in eqn. (1).

(Note that the same typographical error appears in eqn. (5) of ref. 1.) In ref. 3 the error is equating Q_2 in eqn. (A2.3) with Q_2 in eqn. (A2.2). The error propagates to eqn. (A2.9), which they use in subsequent analysis.

In their derivation leading to their regression analysis for "exact" determination of excess energy in Appendix 4 of ref. 3, PF include correctly (except for a typographical error in the definition that they make in eqn. (A3.10), where the vapor term is multiplied by I twice, and the improper inclusion of several minor terms as discussed in Appendix A) the effect of both cell voltage and vapor pressure changes. On p. 341 of ref. 3 they indicate that they determine their correction parameter Ψ/θ^0 by fitting it to the experimentally observed change in cell potential. This would have the effect of removing the vapor term from the calibration, even if the correction is treated properly in their analysis.

To be more explicit about the error in excess energy in the approximate calculation used by PF, we write

$$\begin{aligned} Q_f &= Q - Q_{in}(\text{net}) \\ &= k'_R\left(T_{c_0}^4 - T_b^4\right) - I(E - E_{tn}^c - B) \\ &= Q_f(\text{PF}) - \Delta \end{aligned} \tag{6}$$

where, neglecting small corrections for conductive versus radiative effects, which will be discussed later,

$$Q_f(\text{PF}) = \frac{P_h\left(T_{c_0}^4 - T_b^4\right)}{T_{c_2}^4 - T_{c_1}^4} \tag{7}$$

and, using eqn. (4),

$$\Delta = I\left[(E_2 - E_1) - (B_2 - B_1)\right]\frac{T_{c_0}^4 - T_b^4}{T_{c_2}^4 - T_{c_1}^4} + IB \tag{8}$$

where the negligible effect of E_{tn}^c is not included and we follow PF in assuming that $Q_{f_2} = Q_{f_1}$. From eqn. (A3.10) in ref. 3, correcting the errors noted above gives

$$\frac{\Psi}{\theta^0} \equiv \frac{dE}{dT} - \frac{dB}{dT} \tag{9}$$

For $T_{c_2} - T_{c_1}$ small,

$$\Delta = I\frac{\Psi}{\theta^0}(T_{c_2} - T_{c_1})\frac{T_{c_0}^4 - T_b^4}{T_{c_2}^4 - T_{c_1}^4} + IB \approx I\frac{\Psi}{\theta^0}(T_{c_0} - T_b) + IB \tag{10}$$

This is the form of the term by which PF overestimate Q_f in their approximate analysis.

For comparison, we consider their non-linear regression analysis in Appendix 5 of ref. 3. The first two terms in the numerator of eqn. (A5.1) are

$$\left(E_c - \frac{\Psi}{\theta^0}\,\Delta\theta' - E_{tn}^c\right)I + Q_f \tag{11}$$

where

$$\Delta\theta' \equiv T_c - T_{c_0} = (T_c - T_b) - (T_{c_0} - T_b) \tag{12}$$

Substituting eqn. (12) in statement (11) and regrouping the terms give

$$I(E_{c_0} - E^c_{tn_0}) + Q_f - \frac{\Psi}{\theta^0}(T_{c_0} - T_b)I + \frac{\Psi}{\theta^0}(T_c - T_b)I \tag{13}$$

The first two terms are included in the β_1 parameter in their subsequent analysis. This parameter is used to obtain a value for Q_f, which they acknowledge does not include credit for vapor loss *IB*. The third term in statement (13) is the same as the first term in eqn. (10). Since this term is a constant, it would have been logical to include it in β_1, where it would be used in determining Q_f. However, it was included in their β_2 $\Delta\theta'$ parameter. There is no way to know from the subsequent description of their procedures how the constant and variable parts of $\Delta\theta'$ were separated. It is worth noting that, if $\Delta\theta'$ were treated as $\Delta\theta$, the result would be to overestimate the value of Q_f by $(\Psi/\theta^0)(T_{c_0} - T_{c_b})$, the same as in their approximate analysis.

As is shown in the next section, using the correct calibration procedure described here significantly reduces the calculated excess heat from that reported by PF. Since the correction involved increases with about the second power of the cell current, much of the systematic excess heat that they report may disappear when the correct calibration is used.

ANALYSIS OF PONS–FLEISCHMANN DATA

Recalculation of excess heat

Because of the paucity of experimental details in their publications, it has been difficult to determine quantitatively the effect of calibration errors on the excess energy reported by PF. Specifically, while they have presented the cell power, they have not reported cell temperatures or calibration heater power. However, in ref. 3, they present pictorial data of their cell temperatures which we have interpreted as exemplified below.

The analysis described here involves our interpretation of how the approximate excess heats reported by PF [1–3] were calculated. This interpretation is based on a careful reading of these publications. Except for some minor uncertainties (noted below), which have only small influence on the conclusions, our procedures are firmly based on the methods described by PF.

The approximate excess heats shown in the tables in the PF publications [1–3] were calculated by them using eqns. (A2.9) and (A2.10) from ref. 3. The procedure that they apparently used was to calculate first a radiative differential heat loss from

$$k'_R(\mathrm{PF}) = \frac{P_h}{T^4_{c_2} - T^4_{c_1}} \tag{14}$$

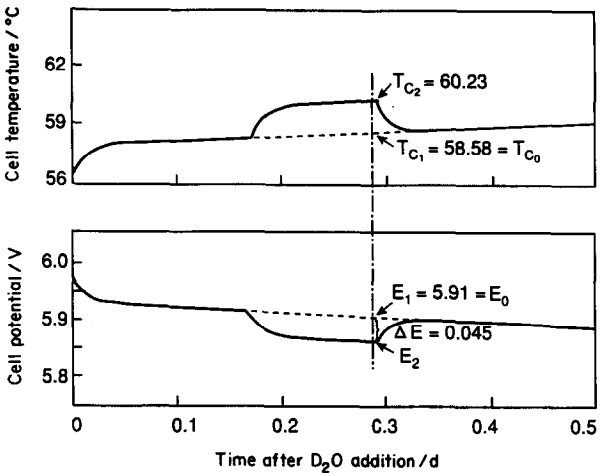

Fig. 1. Schematic representation of Fig. 3A of ref. 3 for a cell operating at 0.8 A in a bath at 29.87°C. The excess energy was reported to be 0.158 W.

from which

$$Q' = k'_{\mathrm{R}}(\mathrm{PF})\left(T_{c_0}^4 - T_{\mathrm{b}}^4\right) \tag{15}$$

is calculated. Following their notation, Q' is used to distinguish it from the Q that they would obtain if they used a mixture of conductive and radiative heat loss. PF estimate a value of Q'/Q slightly less than 1 (see Table A2.1 in ref. 3) and calculate Q, from which

$$Q_{\mathrm{f}} = Q - I(E_0 - 1.54) \tag{16}$$

is calculated. (It is not clear from their discussion whether or not PF use $Q'/Q < 1$ in their calculation, but the effect is small so that it does not significantly affect our results.)

Working backward from these equations and using data from Fig. 3A of ref. 3 (which is reproduced schematically in Fig. 1, using the measurement time near the end of the heater pulse as indicated in their figure caption), the radiative heat transfer coefficient that they used to obtain their excess heat can be calculated from

$$\begin{aligned} k'_{\mathrm{R}}(\mathrm{PF}) &= \frac{[I(E - 1.54) + Q_{\mathrm{f}}](Q'/Q)}{T_{c_0}^4 - T_{\mathrm{b}}^4} \\ &= \frac{[0.8(5.91 - 1.54) + 0.158]1}{(58.58 + 273.15)^4 - (29.87 + 273.15)^4} \\ &= 0.99 \times 10^{-9}\ \mathrm{W\ K^{-4}} \end{aligned} \tag{17}$$

TABLE 1
k'_R and Q_f data

Figure in ref. 3 from which data taken	$10^9\, k'_R$ /W K^{-4}		Q_f/W	
	PF	Corrected	From ref. 3	Corrected
3A	0.99	0.81	0.158	−0.43
3B	0.96	0.80	0.178	−0.42
3C	0.92	0.75	0.372	−0.37
4A	1.14	1.02	0.736	0.52
4B	1.21	1.11	0.888	0.65
4C	1.40	1.30	1.534	1.26

where $Q'/Q = 1$ has been assumed. Values of Q'/Q less than 1 would reduce k'_R proportionally.

This value is substantially less than the $(1.3–1.4) \times 10^{-9}$ W K^{-4} values that they report in Fig. 5C of ref. 3. Furthermore, the size of k'_R calculated in this way changes in their experiments. This can be seen in Table 1, which shows the results of analyzing the data in Figs. 3A–3C and 4A–4C of ref. 3.

Table 1 also shows the corrected differential heat transfer coefficients (or, in other terminology, differential cell constants) calculated from these data using the correct procedures discussed in the previous section. To do this, the power into their calibration heater was determined from

$$\begin{aligned} P_h &= k'_R(\mathrm{PF})\left(T_{c_2}^4 - T_{c_1}^4\right) \\ &= 0.99 \times 10^{-9}\left[(60.23 + 273.15)^4 - (58.58 + 273.15)^4\right] \\ &= 0.24 \text{ W} \end{aligned} \tag{18}$$

Equation (4) was then used to obtain the corrected value for k'_R:

$$\begin{aligned} k'_R(\text{corrected}) &= \frac{P_h + I\,\Delta E - I\,\Delta B}{T_{c_2}^4 - T_{c_1}^4} \\ &= \frac{0.24 + 0.8(-0.045) - 0.8(0.00937)}{2.43 \times 10^8} \\ &= 0.81 \times 10^{-9} \text{ W K}^{-4} \end{aligned} \tag{19}$$

where the temperature and voltage values are again from Fig. 3A of ref. 3 and the values for B are calculated for D_2O vapor pressures and atmospheric pressure of 0.84 bar (1500 m (5000 ft) above sea level, the elevation of Salt Lake City). The effects of small changes in E^c_{tn} are neglected here.

An expression for the corrected value of excess heat can readily be obtained by algebraic manipulation of the above equations:

$$Q_f(\text{corrected}) = \frac{Q'/Q}{(Q'/Q)_c}[I(E-1.54)+Q_f] - I(E-1.54) + \frac{I(\Delta E - \Delta B)}{(Q'/Q)_c}\frac{T_{c_0}^4 - T_b^4}{T_{c_2}^4 - T_{c_1}^4} + IB \tag{20}$$

where $(Q'/Q)_c$ is the factor necessary to correct for the conductive component of heat loss based on the corrected k'_R, and Q'/Q is the factor used by PF in their calculation of excess heat Q_f.

A value for Q'/Q could readily be obtained using our results in Appendix B, which show the radiative and conductive components of heat loss to be about equal, and which give a total heat loss in agreement with the data in Fig. 5C of ref. 3. However, the values of k'_R shown in Table 1 are substantially less than these. This difference could be due to a lower electrolyte level, which would leave the ratio of conductive to radiative loss about the same, or it could be due to a better vacuum in the cell jacket, which would substantially reduce the conductive loss. We cannot determine which is the case and choose to make $Q'/Q = (Q'/Q)_c = 1$ for an estimate of excess heat, in which case eqn. (20) becomes

$$\begin{aligned} Q_f(\text{corrected}) &= Q_f + I\,\Delta E\frac{T_{c_0}^4 - T_b^4}{T_{c_2}^4 - T_{c_1}^4} - I\,\Delta B\frac{T_{c_0}^4 - T_b^4}{T_{c_2}^4 - T_{c_1}^4} + IB \\ &= 0.158 - 0.547 - 0.114 + 0.069 \\ &= -0.43\ \text{W} \end{aligned} \tag{21}$$

for the data in Fig. 3A of ref. 3. This and values for the other figures in ref. 3 are also shown in Table 1.

As can be seen in eqn. (21), the correction term for change in cell potential is substantial, more than 0.5 W from Fig. 3A data. The vapor terms are smaller but still significant. Noting that $T_{c_0}^4 - T_b^4 \propto I(E-1.54)$, the correction terms decrease the calculated excess heat by

$$\Delta \propto I^n \tag{22}$$

where $n \approx 2$. Since the PF data in Fig. 12 of ref. 3 show a similar dependence on the current density, it is possible that most of this dependence of excess energy on current density is due to this error in their analysis. PF do not provide enough data to determine this quantitatively.

Evaluation of Pons–Fleischmann control experiments

A critical test of calorimetry is to obtain the heat balance. The data in Table 4 of ref. 3 show that PF have been able to do this within a milliwatt in most of their experiments where no excess heat is expected. However, they indicate in their

TABLE 2
Deviations from the values of Q excess

Row [a]	Cell current /A	Cell input power /W	Inferred range of cell temperatures [b] /°C	Excess heat corrections		
				Credit for vapor loss [c] /mW	Vapor calibration correction [d] /mW	Potential calibration correction [e] /mW
1	0.1	0.212	31.2–31.8	1.5	−0.5	−2
2	0.2	0.479	32.7–34.1	3	−1	−8
3	0.4	1.482	38.4–42.4	10	−7	−47
4	0.8	5.931	60.5–73.1	69	−118	−318
5	1.6	15.70	97.7–121 [f]	> 2000 [f]	< −2000	−1200
11	0.8	3.742	50.2–59.0	38	−48	−201
14	1.6	16.86	101 –125 [f]	> 3000 [f]	< −3000	−1290

[a] Refers to data rows in Table 4 of ref. 3 numbering from the top. All samples shown are 0.1 cm in diameter and 10 cm long.
[b] Calculated from $Q_{input} = k'_R(T_c^4 - T_b^4)$ using $T_b = 30°C$, $k'_R = (1.5 \text{ to } 1.0) \times 10^{-9}$ W K^{-4} and the indicated input power.
[c] From the IB term in eqn. (21).
[d] From the $I\Delta B$ term in eqn. (21).
[e] From the $I\Delta E$ term in eqn. (21).
[f] Energy removed by evaporation would significantly reduce the inferred temperature.

papers [1–3] that they do not correct their results for vapor loss or cell potential changes during calibration. On the assumption that this is the case, significant deviations from the values of Q_{excess} that they report in their control experiments would be expected. These are shown in Table 2 for several corrections, where the corrections are calculated from eqn. (21) using the low end of the inferred temperature range and a 2°C temperature increase during the calibration. $\Delta E = -0.03$ V was used.

As can readily be seen from Table 2, significant corrections should be made. The dominant correction is that for cell potential changes during calibration. The vapor loss credit is larger than the vapor calibration correction at low temperatures but the situation reverses at higher temperatures. Even the vapor loss credit that PF recognize but do not correct for would lead to significant calculated excess energy in their control experiment if it were included in their calculations, e.g. in Table 4 of ref. 3. Failure to make such large corrections should result in non-zero excess energy in their control experiments. The low excess energy values that they report are unrealistic.

Finally, the very high temperatures inferred for rows 5 and 14 in Table 2 are inconsistent with the experimental cells that they describe. At the input powers that they report and the heat loss rates of their cells, the electrolyte would boil if it were not for the evaporative cooling, which they state is neglected in their calculation. In this temperature range, all the corrections become very imprecise and very large.

OUR EXPERIMENTAL RESULTS

We have conducted an extensive series of experiments. Some of them used palladium rods from the same source as those of PF, that were prepared in the same way. In some of the experiments, the calorimetry used cells and procedures of the type used by PF. (The characteristics of these cells are described in Appendix B.) No excess heat was found in these experiments.

In other experiments, foamed insulation was used to avoid radiation effects. Some of the experiments were open cells, and others were sealed with recombination catalysts to recover the electrolysis enthalpy. A flow cell was also used and is described in Appendix C.

Various palladium cathodes were used: as received from the supplier; cold worked; vacuum annealed and cooled in deuterium; remelted and chill cast; and a 35% porous cathode. Most of the cathodes were in the shape of rods, but other configurations were used, including square sections, a hollow cylinder, v-grooved material and palladium sheet. The anodes were usually platinum, although nickel and gold were used in some experiments.

Most of the experiments used 0.1 M LiOD, but more concentrated solutions were also used. A 2.3 M D_2SO_4 solution was also used in one experiment.

For most experiments the anode was symmetrically arrayed around the cathode. However, in some experiments, asymmetry was intentionally introduced. The current density at the cathode ranged from a few milliamperes per square centimeter to 0.5 A cm^{-2}. The experiments were run for varying lengths of time, but certainly long enough in many cases to load the palladium with deuterium based on diffusion times. Definitive measurements of the level of loading achieved were not made.

Within experimental error, no excess energy was found in any of our experiments. A few experiments were monitored carefully for γ-ray and neutron production. The radiation monitor methods ranged from simple BF_3 counters for neutron detection, to γ spectrometers for secondary-γ detection, to various activation foils and $Mn(NO_3)_2$ solution for the integration of γ signals. In general, the BF_3 counters counted perhaps 4 to 6 neutrons h^{-1} at a counting efficiency of about 0.2%. Three γ counters were used: a 1 in (2.54 cm) NaI crystal monitor, a more sensitive 2 in NaI crystal detector, and a high resolution Ortec intrinsic germanium detector with a 40% sensitivity relative to NaI. The latter was used in conjunction with a Canberra γ spectrometer of outstanding stability. Our resolution was typically 0.002 MeV or better with this instrument. Typically several hundred counts were indicated over a 24 h period in the energy range of secondary γ-rays imputedly from (n,p) reactions in the water bath surrounding the various cells. However, these did not vary significantly from the background level over the course of any observation in which one or more cells were operating. In addition, we used activation foils as the final arbitrator of radiation. These foils were of gold, copper, manganese and indium. All these elements have appreciable cross-sections for neutron absorption and decay with well-characterized γ radiation at

half-lives of 2.694 days, 12.7 h, 154.2 min and 54 min respectively. By encapsulating these foils in a cadmium sheath (which has a large cross-section for the absorption of thermal, but not fast, neutrons) we were also able to monitor any imputed fusion neutrons at 2.45 MeV. The manganese nitrate solution was used in a manner similar to the foils, as described in Appendix C. The foils were counted in low radiation background caves [7]. No radiation was measured outside the expectation values. Nothing above background was found. Many of the electrolytes were checked for tritium build-up. No increase above concentration by electrolysis was found, nor was the concentration of He^4 in the palladium rods found to be above background.

In our isoperibolic calorimetry, the uncertainty in our measurements was at best 5–10% of the input power. These uncertainties are greater than those claimed by PF. However, our measurements could readily have detected excess energies of the size recalculated by us for some of the PF results described in the previous section.

CONCLUSIONS

In this paper we have presented a detailed analysis of the thermodynamics and calibration of open calorimetric cells of the type described by PF. We have used this analysis to show that in their approximate procedures they neglected at least two important effects in ascertaining the rate of heat loss from their cells. One is the reduction in resistance (and hence changed operating power) of the cell due to the heating caused by the differential calibration heater. The other is evaporative cooling of the electrolyte, which becomes important at higher cell operating temperatures (above 60°C) and is also increased by the calibration heater. Neglect of either of these effects leads to an overestimate of the rate of heat loss from the cell (i.e. leads to falsely implied excess heat generation within the cell). We have computed the magnitude of the errors caused by neglect of these effects in the PF data [1–3], and in some cases the errors are greater than their inferred "excess heat". In some instances, excess heat still remained after correcting for these errors. We also show that the null results that PF obtain in their light-water control experiments are invalidated by the magnitude of these errors. We do not show that these errors overwhelm all their excess heat claims, e.g. the large transient heat "bursts" which they present.

Our analysis of the PF data implies that the strong current dependence of their claimed excess heat is likely also to be an artifact of the calibration errors. Since their regression analysis of their cell operation yields the same excess energy as their approximate method, we conclude that it is similarly flawed. We have analyzed the nature of the heat loss in a PF-type cell and have found that it is about half radiative and half conductive, which cautions against assumptions of all-radiative coupling.

We have summarized our various calorimetric experiments, some of which were quite similar to the PF experiments and cells and some of which were not. The

experiments utilized various cathodes and electrolytes and employed both open and closed cells. We have given a detailed description of our closed-cell experiments, since these differ the most from the PF design. We observed no excess heat generation greater than 5% of the input energy. In addition, no neutrons, photons, helium isotopes, or tritium in excess of experimental uncertainty were observed in any of these experiments.

In summary, we have not been able to find any evidence for excess heat generation in the electrolysis of D_2O using palladium cathodes. While we cannot disprove all the claims of PF to have achieved excess heat generation, our analysis of the PF data [1–3] shows that, if they used the procedures that they describe to obtain their approximate excess heat, they neglect effects that significantly reduce the excess heat produced in their experiments.

ACKNOWLEDGMENTS

We gratefully acknowledge the contributions of our colleagues Gary Renlund, Woodfin Ligon, Joe Salvo, Frank Mondello, Hans Grade, Frank Ciani, Les String and Don Sorensen, for their assistance in sample preparation and analysis, and in experimental design and construction.

REFERENCES

1 S. Pons and M. Fleischmann, Fusion Technol., 17 (1990) 669.
2 S. Pons and M. Fleischmann, Proc. 1st Annu. Conf. on Cold Fusion, Salt Lake City, UT, 28–31 March, 1990, p. 1.
3 M. Fleischmann, S. Pons, M.W. Anderson, L.J. Li and M. Hawkins, J. Electroanal. Chem., 287 (1990) 293.
4 M. Fleischmann, S. Pons and M. Hawkins, J. Electroanal. Chem., 261 (1989) 301.
5 M. Fleischmann, S. Pons and M. Hawkins, J. Electroanal. Chem., 263 (1989) 187.
6 F.T. Wagner, T.E. Moylan, M.E. Hayden, U. Narger and J.L. Booth, J. Electroanal. Chem., 295 (1990) 393.
7 L.N. Lewis, P.G. Kosky and N. Lewis, J. Radioanal. Nucl. Chem. Lett., 145 (2) (1990) 81.

APPENDIX A: THERMODYNAMICS OF AN OPEN ELECTROCHEMICAL CELL OF THE PONS–FLEISCHMANN TYPE

The "black-box" model of Pons, Fleischmann and co-workers (PF) [A1–A3] is the major result of a thermodynamic analysis of their calorimeter. In its general form [A1] before simplification it is expressed as their eqn. (9). Subsequent modifications and simplifications depend on the veracity of this equation. It was derived from considerations shown as Fig. 3A of ref. A1. The result is reproduced

below with its original nomenclature:

$$C_{P,D_2O,l}\left(M^0-(1+\beta)\frac{\gamma It}{2F}\right)\frac{d(\Delta\theta)}{dt}-C_{P,D_2O,l}(1+\beta)\frac{\gamma I\,\Delta\theta}{2F}$$

$$=[E_{cell}(t)-\gamma E_{thermoneutral,cell}]I+Q_f(t)+\Delta QH(t-t_1)-\Delta QH(t-t_2)$$

$$-\frac{\gamma I}{F}\left[\left(0.5C_{P,D_2}+0.25C_{P,O_2}+\frac{0.75P}{P^*-P}C_{P,D_2O,v}\right)\Delta\theta+\frac{0.75P}{P^*-P}L\right]$$

$$-k_R'^0\left(1-(1+\lambda)\frac{\gamma It}{2FM^0}\right)\left[(\theta_{bath}+\Delta\theta)^4-\theta_{bath}^4\right] \qquad \text{(A1)}$$

Unfortunately their derivation is imprecise; in several relatively minor ways their "black-box" system is inconsistent with formal thermodynamics. However, since some of the claimed excess heats are themselves small, it is necessary to determine whether the magnitude of errors introduced by the incorrect terms vitiates any of their conclusions.

A formal thermodynamic system consists of a boundary to a control volume within which certain energetic events occur and across which work, mass and enthalpy terms may flow. The first law of thermodynamics simply relates the energy changes within the control volume to heat and enthalpy flows crossing its boundaries. We seek a derivation that contains a minimum number of (explicitly stated) approximations. These relate only to properties within the control volume, specifically the state of the Pd–D_2 system and to LiOD–D_2O solution. As will be seen, the majority of errors of PF are not large in an absolute sense, but they do generate uncertainties which, in our view, tend to be in conflict with their claimed error bars. The most serious error is an unsteady term in the heat capacity of absorbed palladium; however, even this is only a few tenths of a per cent.

Consider the thermodynamic system shown in Fig. A1. In this thermodynamic analysis we can define exactly what occurs within the control volume (broken boundaries in Fig. A1) and what crosses the boundary walls. In this case what goes into the system is work via the voltage drop E to pass the current I through the cell. No other thermodynamic quantity passes into this system. We shall eventually show a self-consistent derivation of $E_{thermoneutral,cell}$ and the relevant reference states of it and other thermodynamic terms as necessities of the derivation, and not its artificial constructs.

We have to deal with quantities inside the control volume; so we cannot use a strict "black-box" treatment. Specifically, deuterium is occluded into the palladium; this is an energetic process and the heat of solution of the D_2 in the palladium should be accounted for in a consistent manner. As an approximation we can separate the terms into a palladium component and an absorbed D_2 component; it is useful to make this artificial separation because data are conveniently available for each of the constituent terms. We write the reaction of

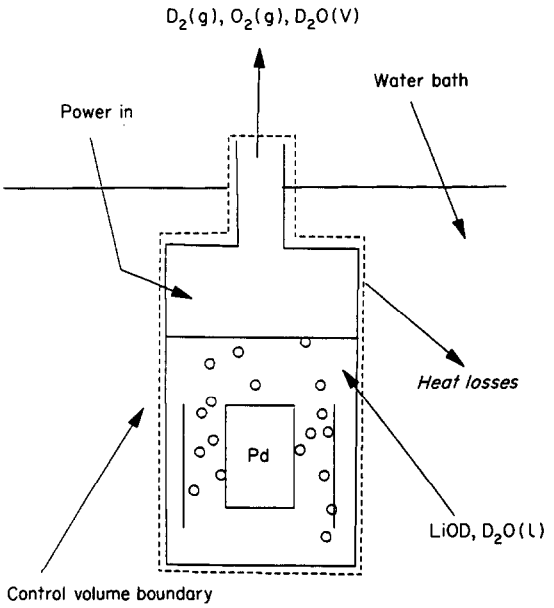

Fig. A1. Thermodynamic boundary for open-electrochemical-cell system.

deuterium within the palladium as

$$D_2(g) \leftrightarrow D_2(g:s) \tag{A2}$$

for which $\Delta H^s = h^s_{D2} - h_{D_2} \approx -35.2$ kJ per mole of D_2 gas (ref. A4, p. 125) and serves to define the enthalpy $h^s_{D_2}$ of the deuterium within the palladium matrix.

We assume that the faradaic reaction which occurs is

$$D_2O(1) \rightarrow D_2(g) + 0.5O_2(g) \tag{A3}$$

for which the standard enthalpy of reaction is ΔH^0_R. However the standard datum of 298.15 K is not the reference temperature in this instance. PF [A1] in their eqn. (9) used the cell temperature as a datum; later, in their eqn. (11) they used the bath temperature as a datum. There is, of course, a simple relationship between the reaction heats ΔH^b_R and ΔH^c_R given by Kirchhoff's equation:

$$\Delta H^c_R = \Delta H^b_R + \int_{\theta_b}^{\theta_c} (C_{p,D_2} + 0.5C_{p,O_2} - C_{D_2O,l})\, d\theta \tag{A4}$$

We shall write $C_{p,D_2} + 0.5C_{p,O_2} - C_{D_2O,l}$ as ΔC and assume that it is independent of θ so that

$$\Delta H^c_R = \Delta H^b_R + \Delta C\, \Delta\theta \tag{A5}$$

where $\Delta\theta = \theta_c - \theta_b$.

The energy losses from the cell consist of the heat leakage through its walls (mostly to the thermostatic water bath), some additional heat leaks to the atmosphere through its lid, and some enthalpy loss through convection of $D_2(g)$, $O_2(g)$ and $D_2O(v)$ through the vent to atmosphere. All these cross the system with the broken control volume boundaries shown in Fig. A1. The first law states that

rate of change in the control volume enthalpy

= power in + excess heat within the control volume − heat loss rate

− net convected enthalpy

which is mathematically expressed by

$$\frac{d}{dt}\left(m_l h_l + \sum m_s h_s + m^s_{D_2} h^s_{D_2}\right) = EI + Q_f(t) - Q - \dot{m}_{D_2} h_{D_2} - \dot{m}_{O_2} h_{O_2} - \dot{m}_v h_v \tag{A6}$$

where m_i is the number of moles of species i within the control volume, $\dot{m}_i$ is the molar rate at which i crosses the boundary of the control volume, and h_i is the molar enthalpy of species i. On the left-hand side, terms involve the enthalpy of the liquid phase within the cell and the enthalpy (or, effectively, internal energy) changes of inert solids such as the quartz cell and associated hardware and inclusive of the palladium matrix but exclusive of absorbed D_2. The latter has been separated as the term $m^s_{D_2} h^s_{D_2}$. The subscript l refers to the $D_2O(l)$ which is in the cell at any instant (in fact the 0.1 M LiOD solution, for which both the heat of solution and its concentration dependence are being neglected), the subscript D_2 to the vented deuterium gas, the subscript O_2 to the vented oxygen gas and the subscript v to the evaporated $D_2O(v)$ vapor which is swept out with the electrolyzed gases. All vented gases and vapors are assumed to be at the cell temperature θ_c. At steady state, i.e. at constant cell temperature within the control volume, all left-hand side terms except the depletion of the $D_2O(l)$ are identically zero.

The initial inventory of D_2O is the sum of the heavy water remaining at time t, the heavy water which has been electrolyzed to the $D_2(g)$ (and either vented or stored within the palladium), and the heavy water that has evaporated. Thus, if at any instant the present inventory of heavy water is m_l and the total evaporated water is m_v,

$$m_{initial} = m_l + m_{le} + m_v \tag{A7}$$

in which the subscript le refers to liquid which has been electrolyzed. Then, differentiating with respect to time gives

$$\dot{m}_l = -\left(\dot{m}_{le} + \dot{m}_v\right) \tag{A8}$$

and

$$\dot{m}_{le} = \dot{m}_{D_2} + \dot{m}^s_{D_2} \tag{A9}$$

Equation (A9) expresses the fact that every mole of water which has been

electrolyzed has been either vented as a mole of D_2 at a molar rate $\dot{m}_{D_2}$ or stored in the palladium lattice as D_2 at a rate of $\dot{m}^s_{D_2}$.

On the assumption that process (A3) is 100% faradaic ($\gamma = 1$ in the PF treatment),

$$2\dot{m}_{O_2} = \dot{m}_{D_2} + \dot{m}^s_{D_2} = \frac{I}{2F} \tag{A10}$$

in which F is Faraday's constant and equal to 96 485 C mol^{-1}.

Then, performing the implied differentiation on eqn. (A6) and using the molar balances (A8)–(A10), we obtain

$$\left(m_1 C_1 + \sum m_s C_s + m^s_{D_2} \frac{dh^s_{D_2}}{d\theta_c}\right) \frac{d\theta_c}{dt} + \dot{m}^s_{D_2}(h^s_{D_2} - h_{D_2})$$

$$= EI + Q_f - Q - \frac{I}{2F}(h_{D_2} + 0.5h_{O_2} - h_l) - \dot{m}_v(h_v - h_l) \tag{A11}$$

where C_i is the heat capacity of the condensed phase i. The terms on the left-hand side of the equation are those associated with the transient response of the cell. Several terms in eqn. (A11) can be cast in more familiar forms. The derivative of the enthalpy term in large parentheses which consists of the thermal response of the deuterium in the palladium can be simplified:

$$\frac{dh^s_{D_2}}{d\theta_c} \Delta C^s_{D_2} \approx 29 \text{ J K}^{-1} \text{ mol}^{-1} \tag{A12}$$

This identity defines a heat capacity equivalent to the absorbed deuterium in the palladium. In the absence of better information we have estimated it using data for protium (ref. A4, p. 40). Further, if we define R as the ratio of deuterium to palladium, then

$$m^s_{D_2} = 2Rm_{Pd} \tag{A13}$$

Other terms in eqn. (A11) can also be clarified. The term $h_{D_2} + 0.5h_{O_2} - h_l$ is simply the enthalpy ΔH^c_R, of reaction (A3) taken at the cell temperature θ_c.

Similarly, $h^s_{D_2} - h_{D_2}$ is the enthalpy ΔH^c_s of reaction (A2) taken at the cell temperature. Likewise the term $h_v - h_l$ is the latent heat L^c of vaporization measured at the cell temperature; it may be corrected to bath temperature if desired by a Kirchhoff-type correction:

$$L^c = L^b + \delta C \, \Delta\theta \tag{A14}$$

where $\delta C = C_{p,D_2O(v)} - C_{p,D_2O(l)}$.

The molar rate terms $\dot{m}^s_{D_2}$ and $\dot{m}_v$ can also be simplified to useful expressions. The palladium cathode may or may not be in thermal and/or chemical equilibrium with its surroundings. If its hydrogen content is controlled by mass transport, thermodynamics is effectively disconnected from the mass flow of hydrogen into and out of the palladium.

The term $\dot{m}_v$ can also be simplified by assuming the gases exiting the cell are saturated with heavy-water vapor. Then

$$\frac{\dot{m}_v}{\dot{m}_v + \dot{m}_{D_2} + \dot{m}_{O_2}} = \frac{P}{P^*} \tag{A15}$$

in which P is the vapor pressure of a saturated vapor of 0.1 M LiOD in $D_2O(l)$ measured at the cell temperature and P^* is the atmospheric pressure. P is approximated by the vapor pressure of $D_2O(l)$.

Hence using the molar balance in eqn. (A10) gives

$$\dot{m}_v = \frac{3I}{4F}\frac{P}{P^* - P} \tag{A16}$$

if we ignore the correction $\dot{m}^s_{D_2}$ to the correction $\dot{m}_v$.

The transient first-law balance then reads

$$\left(m_1C_1 + \Sigma m_sC_s + 2Rm_{Pd}C^s_{D_2}\right)\frac{d\theta_c}{dt} + \dot{m}^s_{D_2}\,\Delta H^s$$
$$= EI + Q_f - Q - \frac{I}{2F}\,\Delta H^c_R - \frac{3I}{4F}\frac{PL^c}{P^* - P} \tag{A17}$$

Finally, the thermoneutral potential of reaction (A3) at the cell temperature can be defined as

$$E^c_{tn} = \left|\frac{\Delta H^c_R}{2F}\right| = \left|\frac{\Delta H^b_R + \Delta C\,\Delta\theta}{2F}\right| \approx 1.53\ \text{V} \qquad \text{at } 25°\text{C} \tag{A18}$$

so that

$$\left(m_1C_1 + \Sigma m_sC_s + 2Rm_{Pd}C^s_{D_2}\right)\frac{d\theta_c}{dt} + \dot{m}^s_{D_2}\,\Delta H^s$$
$$= I(E - E^c_{th}) + Q_f - Q - \frac{3I}{4F}\frac{PL^c}{P^* - P} \tag{A19}$$

In principle, the term $\dot{m}^s_{D_2}\,\Delta H^s$ could be cast into a pseudo-heat capacity term such as those within parentheses. If the deuterium is in thermal equilibrium at all times in the palladium, as the cell temperature is raised, it represents an endotherm; as the cell temperature is lowered, it represents an exotherm. Thus, in thermal equilibrium it behaves as if it is another heat capacity term. However, it could behave in an opposite sense if it were decoupled by the mass transfer lag within the palladium. It would be possible to use either the equilibrium or the mass-transfer-limited case if numerical estimates are needed for this term.

COMPARISON WITH PONS–FLEISCHMANN DATA

Equation (A19) is directly equivalent to eqn. (9) in ref. A1 (for $\gamma = 1$ and neglecting the unit-step calibration pulse). They are compared in Table A1. The

TABLE A1
Comparison of energy terms

PF	This work
$\frac{d(\Delta\theta)}{dt}$	$\frac{d\theta_c}{dt}$
$C_{P,D_2O,l}(M^0-(1+\beta)\frac{It}{2F})$	$m_1C_1+\Sigma m_sC_s$
$E_{cell}(t)$	E
$E_{thermoneutral,cell}$	E_{tn}^c
$Q_f(t)$	Q_f
$\frac{0.75PLI}{F(P^*-P)}$	$\frac{3IPL^c}{4F(P^*-P)}$
$k_R'^0[1-(1+\lambda)\frac{It}{2FM^0}][\theta_{bath}+\Delta\theta)^4-\theta_{bath}^4]$	Q
–	$2R_{Pd}C_{D_2}^s\frac{d\theta_c}{dt}$
–	$\dot{m}_{D_2}^s\Delta H^s$
$(0.5C_{P,D_2}+0.25C_{P,O_2}-0.5C_{P,D_2O,l})\frac{I\Delta\theta}{F}$	–
$C_{P,D_2O,l}\frac{\beta I\Delta\theta}{2F}$	–
$\frac{0.75PC_{P,D_2O,v}I\Delta\theta}{F(P^*-P)}$	–

first seven rows of pairs are basically identical except for trivial, nomenclature or second-order terms. For example, the term $m_1C_1+\Sigma m_sC_s$ is identically the cell heavy-water thermal equivalent, which at zero time (and for $\beta\equiv 0$), is $C_{P,D_2O,l}M^0$ (the neglected term in β was to account for non-faradaic heavy-water losses as evaporation occurs in the cell). The factors involved in the heat leak term Q are discussed in Appendix B. For the purposes of Table A1, it may be taken as identical with the expanded form used by PF.

In fairness to PF, it must be stated that this table does not represent a unique deconvolution of their analysis. Other term-by-term interpretations are possible; by changing the reference temperature, minor specific heat terms (via Kirchhoff corrections) can be introduced. The Kirchhoff-correction term used by PF,

$$I(0.5C_{P,D_2}+0.25C_{P,O_2}-0.5C_{P,D_2O,l})\frac{\Delta\theta}{F}$$

is identical to $(I\,\Delta C\,\Delta\theta)/(2F)$ but is incorrect in the context of this deconvolution

TABLE A2
Comparison of energy balance with the Pons–Fleischmann "black-box" thermodynamics approach

PF	This work	Energy/W
Steady state energy terms		
$T_{cell} = 37°C$		
$\frac{I\Delta\theta}{2F}$	–	−0.001
$\frac{IC_{P,D_2O,l}\beta\,\Delta\theta}{2F}$	–	2×10^{-4}
$\frac{0.75IPC_{P,D_2O,v}\,\Delta\theta}{F(P^*-P)}$	–	6×10^{-5}
$T_{cell} = 65°C$		
$\frac{I\Delta\theta}{2F}$	–	−0.001
$\frac{0.75PIC_{P,D_2O,l}\,\Delta\theta}{F(P^*-P)}$	–	0.002
$\frac{IC_{P,D_2O,l}\beta\,\Delta\theta}{2F}$	–	0.004
Unsteady state energy terms		
–	$2Rm_{Pd}C^s_{D_2}$	0.5% of $C_{p,D_2O,l}M^0$
–	$\dot{m}^s_{D_2}\Delta H^s$	5.8×10^{-5}

since it is already included in the thermoneutral potential taken at the cell temperature. Each of the heat capacity terms in the last three rows in the first column are simply incorrect, because the "black-box" approach to the thermodynamic balance used implicit assumptions for the form of certain terms in the formulation, not deductions from strict adherence to the first law. Later, in eqn. (11) of ref. A1, the reference state of the thermoneutral potential to the bath temperature is changed and then, in consequence, several (small) heat capacity terms are incorrectly subtracted.

The basis of the latent heat term L is not defined by PF. In Table A1 it is assumed that they referenced L to the cell temperature (at which the evaporation is occurring), but it could have been the bath temperature. However, some other small terms would then be changed from eqn. (9) of ref. A1. Indeed, several analogues to Table A1 would be equally valid; but eqn. (9) of ref. A1 is essentially different from eqn. (A19) above in several irreducible ways. In a pragmatic sense it is necessary to ask which of these small terms are significant in magnitude. Table A2 compares eqn. (A19) term by term with eqn. (9) of PF for the steady state and

for the unsteady state. The discrepancies are small (although not necessarily within the error bars claimed by PF). In constructing Table A2, several simplifications have been made. In the absence of additional experimental details, the bath temperature is 30°C, $\Delta\theta = 7$°C and 35°C (thus the cell temperatures are 37°C and 65°C corresponding respectively to about 1 W and 5 W input to the cell), $I = 0.4$–0.8 A, $R = 1$, $\dot{m}^{s}_{D_2} = 1.6 \times 10^{-5}$ mol s^{-1} and $\beta = 1.5P/(P^* - P)$. The last pair of values are based on experimental data obtained in this laboratory and secondly by comparing the time derivative of the PF term $(C_{P,D_2O,l}\beta\ \Delta\theta)2F$ with $\dot{m}_v$.

The term $2Rm_{Pd}C^{s}_{D_2}\ d\theta_c/dt$ has not been reduced to "watts" since this would involve a specification of $d\theta/dt$; its thermal capacity component is therefore compared with the thermal capacity of the system. We have assumed 50 g of heavy water as the basis of the thermal equivalence of their cell.

REFERENCES FOR APPENDIX A

A1 S. Pons and M. Fleischmann, Fusion Technol., 17 (1990) 669.
A2 S. Pons and M. Fleischmann, Proc. 1st Annu. Conf. on Cold Fusion, Salt Lake City, UT, 28–31 March 1990, p. 1.
A3 M. Fleischmann, S. Pons, M.W. Anderson, L.J. Li and M. Hawkins, J. Electroanal. Chem., 287 (1990) 293.
A4 F.A. Lewis, The Palladium–Hydrogen System, Academic Press, London, 1967.

APPENDIX B: HEAT LOSS FROM THE PONS–FLEISCHMANN-TYPE CELL

The cell under consideration and its approximate dimensions are shown in Fig. B1. In operation the cell is immersed in a water bath up to the intersection of the inner and outer glass jackets. The space between the inner and outer glass is evacuated to some unspecified pressure. Electrolyte fills the inner glass tube to some distance below the intersection. This distance varies in time as the water in the cell is electrolyzed. The space above the electrolyte is filled with electrolysis product gases and the vapor from the electrolyte. This space is not sealed so that these gases can escape as they are generated; however, the escape paths are long and narrow enough so that air does not diffuse into the cell at an appreciable rate. Calculated and measured heat losses for this type of cell are discussed and compared in this appendix.

Paths for heat loss

There are four available paths for heat loss from the electrolytic cell. One is radiation from the outer surface of the inner cylinder. Another is thermal conduction through the space between the inner and outer cylinders. A third is thermal conduction out of the top through the cylinder walls, tubes and wires inserted through the Kel-F plug and through the gas space at the top. The fourth is the heat removed by the flow of gases out of the cell. (This fourth loss, discussed in previous sections on cell calibration and analysis of PF data, becomes significant at

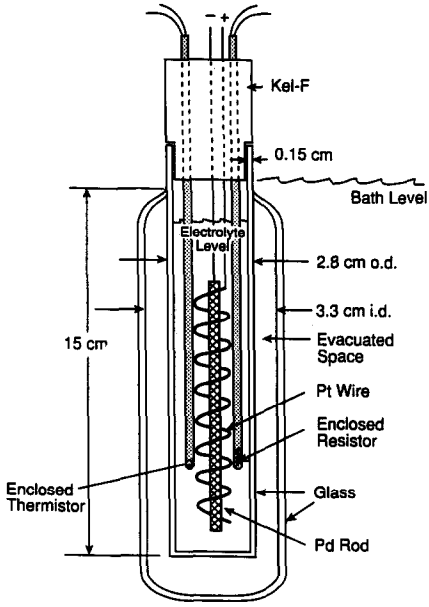

Fig. B1. Schematic view of the cell used showing approximate dimensions.

temperatures higher than about 60°C. Only the other three heat loss processes are considered here.)

The upper limit of radiation loss is obtained by assuming that the emissivity of the glass surfaces in the cell is equal to unity for the wavelengths that are important. This should be a good assumption for glass at 300 K. In that case the rate of radiant energy loss is

$$Q_r = \sigma\left(T_c^4 - T_b^4\right)A_r \tag{B1}$$

where $\sigma = 5.67 \times 10^{-12}$ W cm^{-2} K^{-4}, T_c is the cell temperature, T_b is the bath temperature and A_r is the effective radiating area. For a cell 2.8 cm in outer diameter by 15 cm long, the total area is about 144 cm^2, including top and bottom and the full length of the cylinder. The effective area would be less than that.

The conductance through the evacuated space depends on the pressure and the kind of gas in the space. Once the pressure is low enough to avoid convection in the gas, the thermal conductance of the gas stays constant until the size of the gap between the inner and outer cylinder becomes comparable with the mean free path of the gas molecules. For the 0.5 cm gap, this occurs at pressures somewhat less than 100 mTorr. Above that pressure the thermal conductivity of the gas is

$$Q_c = \frac{k_v}{S}(T_c - T_b)A_c \tag{B2}$$

where S, the vacuum gap between the cylinders, is about 0.5 cm and k_v is the

thermal conductivity of the residual gas in the vacuum. For air, $k_v = 2.68 \times 10^{-4}$ W cm^{-1} K^{-1}.

Thermal conduction out of the top has several paths. Quantitatively, the conduction up the glass cylinder can be most readily determined, because the top of the cylinder at the upper edge of the vacuum jacket is thermostated by the bath. Therefore the heat loss up the cylinder is

$$Q_g = \frac{k_g}{L}(T_c - T_b)A_c \tag{B3}$$

where A_c, the area of the glass cylinder, 2.8 cm in diameter by 0.15 cm thick, is about 1.3 cm^2, $k_g \approx 10 \times 10^{-3}$ W cm^{-1} K^{-1} and L is the distance from the top of the electrolyte to the contact with the bath.

The dimensions of the top gas space preclude convection so that the heat loss is determined by the conductivity of air and the temperature of the Kel-F, which is unknown. In any event, the heat loss is small compared with the other losses. Similarly, heat loss up the wires is found to be small. Including a reasonable amount for these would raise the effective area of the glass from 1.3 to 1.8 cm^2 for the purpose of estimating the heat loss.

Comparison with experiment

A cell of the type used by PF was operated with an electrolyte of 0.1 M LiOH in light water to calibrate the heat loss from the cell. Figure B2 shows the relationship between the power into the cell and the increase in temperature of the cell above bath temperature over an exaggerated temperature range. The figure illustrates the difference between the integral cell constant $(UA)_i = (Q_r + Q_c + Q_g)/(T_c - T_b)$ and the differential cell constant $(UA)_d = d(Q_r + Q_c + Q_g)/dT$, when non-linear processes such as radiation are involved in the heat loss. The integral cell constant, which is simply the net power into the cell divided by the corresponding temperature difference, is used to compare the experimental and calculated heat losses. (The integral cell constant is used here to compare the relative size of the different heat loss components. Calibration of the cell using a differential cell constant and the use of the calibration to determine any "excess energy" are discussed in previous sections.) The data points in Fig. B3 are the integral cell constant as a function of time after the cell was filled so that the electrolyte level was about 1 cm below the intersection between the inner and outer glass cylinders. The bath temperature was 20°C, and the cell temperature was about 30°C. The power into the cell and the cell temperature both changed as the level of the electrolyte changed.

Equations (B1)–(B3) must account for these observed cell constants. As noted above, in an open cell with the electrolysis gas vented, the electrolyte level is constantly changing; so A_r, A_c and L are changing, and the calculated heat loss must fit that change as well as the absolute value of heat loss. Figure B3 shows the calculated values for $Q/(T_c - T_b)$ for the three components of heat loss. The only

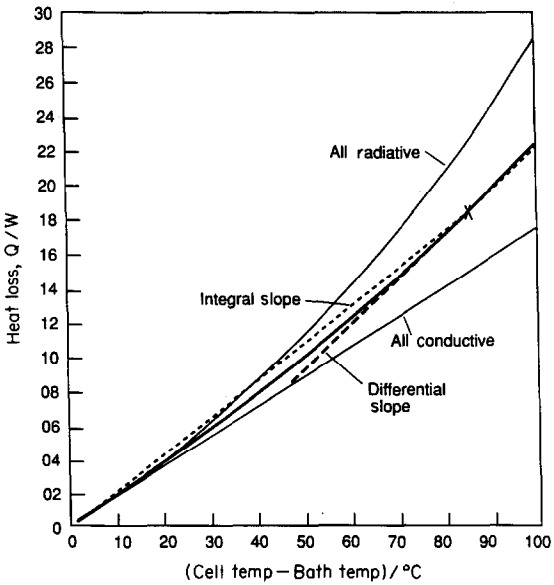

Fig. B2. Heat loss from a cell like that in Fig. B1, shown over an exaggerated range of temperature differences between the cell temperature and bath temperature to illustrate the effect of radiative loss. The bold curve is from experimental results. The difference between the integral and differential slopes caused by a radiative component is shown.

adjustable parameter was the area at $t = 0$, which was chosen to be 139 cm^2 for both A_r and A_c to match the measured cell constant. (The areas should not be exactly the same, but at the level of approximation involved here the difference is not important.) The areas were decreased as a function of time to accommodate the 5.5 ml day^{-1} of H_2O addition required to restore the electrolyte level. (This is somewhat higher than the 4.9 ml day^{-1} loss resulting from electrolysis at 0.6 A. The excess is no doubt due to evaporation and droplets in the vapor caused by bubbling. This 10% volume effect of evaporation translates to a 1.2% evaporative energy loss. The experimental observations were not corrected for this.)

Neither the calculated nor the experimental results described here are intended to be a definitive description of the cell's heat loss characteristics. In spite of the approximations involved, several conclusions can be drawn. First, the radiative heat loss can account for only about one half of the observed heat loss. Second, the full conductivity of air (without convection) in the vacuum space is needed to obtain the observed heat loss. (One monolayer of gas on the inner surface of the vacuum space is enough to raise the pressure to more than 100 mTorr when desorbed; so this is not a surprising result unless the space is very well degassed during evacuation.) Third, the conduction out the top is not trivial and is necessary to fit the slope of the cell constant versus time in the early part of the filling cycle.

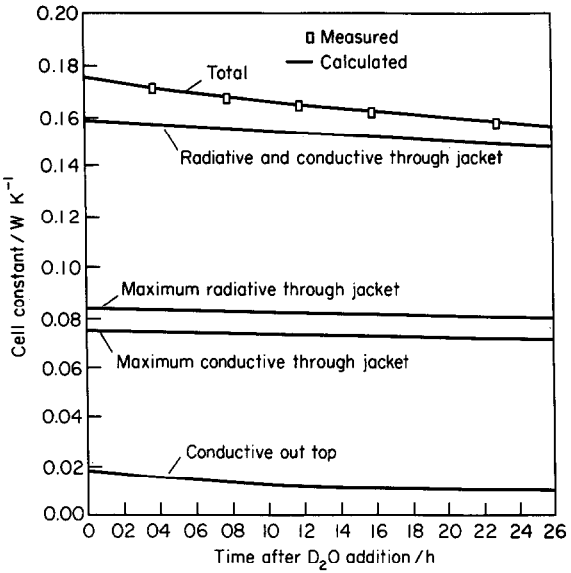

Fig. B3. Change in time of the differential cell constant determined from a change in cell temperature with added resistive heating for a cell of the type shown in Fig. B1 operating at 0.6 A. The full curves are calculated for different components of heat loss using an area at time zero to fit the total calculated cell constant to the measured cell constants.

The bold middle curve in Fig. B2 is calculated from

$$Q = 7.88 \times 10^{-10}(T_c^4 - T_b^4) + 0.0925(T_c - T_b) \tag{B4}$$

The coefficients are those used at $t = 0$ to fit the experimental data in Fig. B3. In the terminology used by PF, $k_R = 7.88 \times 10^{-10}$ W K^{-4} and $k_c = 0.0925$ W K^{-1}. The value of k_R can be compared with the value 7.37×10^{-10} W K^{-4} used by them in ref. 3, p. 313. This implies an effective radiating area of 130 cm^2 in their calculation compared with the area of 139 cm^2 that we used. This is consistent with their total radiative heat loss coefficient $k'_R = 1.5 \times 10^{-9}$ W K^{-4}, compared with a value of about 1.66×10^{-9} W K^{-4} calculated from the values in eqn. (B4). For our results, the ratio ϕ of the two terms in eqn. (B4) discussed in Appendix 2 of ref. 3 is

$$\phi = + \frac{k_c}{4T_b^3 k_R} = 1.06 \tag{B5}$$

for a bath temperature of 30°C while, for their values on p. 313 of ref. 3, $\phi = 1.08$. (Their suggestion there that the radiative cell constant should be increased from 7.37×10^{-10} W K^{-4} to 8.5×10^{-10} W K^{-4} as a result of their analysis in ref. 3, Appendix 4, is incorrect.)

On the basis of these results, we conclude that the values of heat loss discussed here are a good representation of the characteristics of the cells used by PF.

APPENDIX C: CLOSED-CELL ELECTROLYSIS IN THE Pd–D_2 SYSTEM

Apparatus

Many of the uncertainties in open-cell electrolysis systems are avoidable in closed-cell systems. For example, there are no corrections for the convection of chemical enthalpy terms out of the cell or for the uncertainty as to recombination of D_2–O_2 in the head space of the cell. In fact it is mandatory to recombine all the excess gas in the head space of a closed cell to limit its internal pressure.

Figures C1A and C1B are schematics (not to scale) of the cell used in the present study; the materials of construction interfacing the cell's interior were polytetrafluorethylene (PTFE), platinum, palladium, rhodium and an unwetted lid made of polymethylmethacrylate (PMMA), which was sealed against the PTFE cell body by an unwetted Viton O-ring (not shown). The PTFE cell body was supported externally by a close-fitting brass can (Fig. C1A).

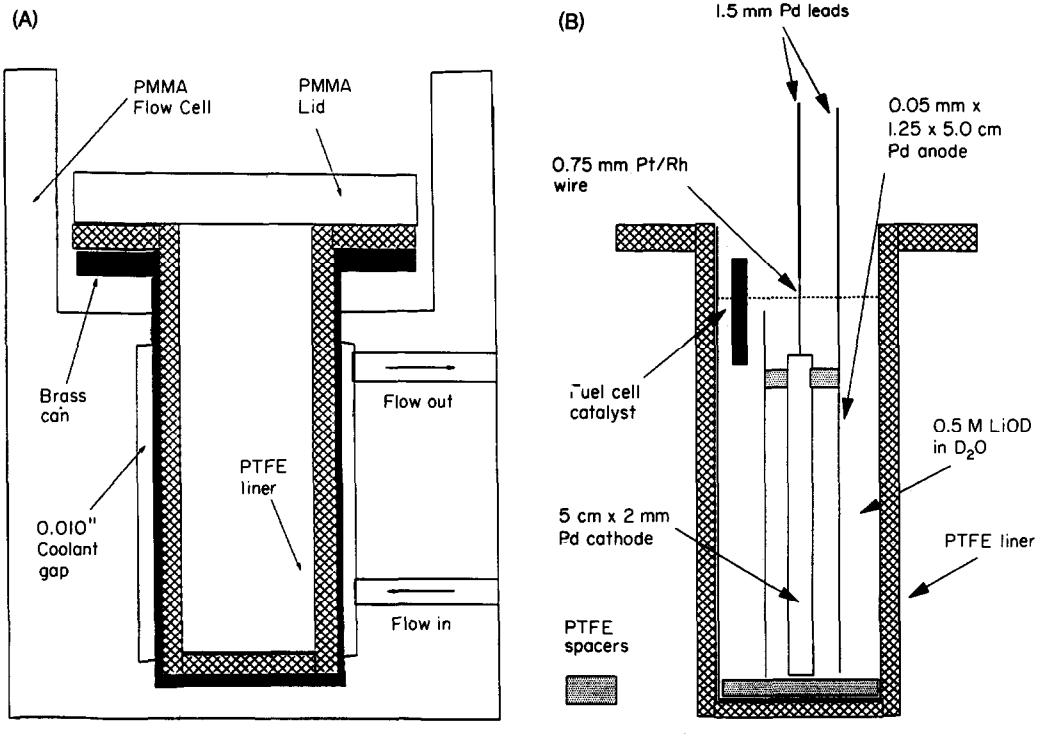

Fig. C1. Schematic diagrams of closed cell showing (A) the coolant path and (B) the interior details.

An important feature of the cell design shown in Fig. C1B is the electrolyte-wetted fuel cell catalyst of platinum mounted on PTFE. It efficiently replenished all the supply of electrolyzed D_2O except for the equivalent of the D_2 adsorbed by the palladium cathode. Since the system was closed, the uptake of D_2 was easily monitored by monitoring the system pressure (i.e. the pressure caused by the stoichiometric equivalent of O_2 corresponding to the adsorbed D_2). A fine PTFE capillary sealed into the lid of the vessel with a PTFE Swagelok fitting served this purpose. The liquid-phase composition was monitored by extracting a liquid sample through a similar (but liquid-submerged) PTFE capillary. A corresponding volume of fresh electrolyte was always returned to the cell to ensure a constant-volume electrolyte. Appropriate external valving allowed the necessary manipulations for sampling the gas, its pressure and the liquid without exposing the cell or its contents to the atmosphere. Samples of withdrawn liquid showed no statistically significant tritium above the original content, nor did samples of the gas phase indicate the presence of anomalous amounts of helium as determined by high resolution mass spectrometry.

The cathode (Fig. C1B) was a piece of palladium rod 2.01 mm in diameter by 5.0 cm long purchased from the Johnson Matthey Company. It was spot welded to 10 cm of Pt–Rh wire 0.030 in in diameter, which in turn was welded to a long palladium rod $\frac{1}{16}$ in in diameter. The Pt–Rh wire was used to avoid the possible diffusion of deuterium from the cathode if the palladium rod had been directly attached to the cathode. The palladium rod was sealed through the cell lid in a $\frac{1}{16}$ in PTFE Swagelok fitting.

The palladium cathode had been pre-loaded with D_2 in an especially constructed quartz furnace which was evacuated to a pressure of a few millitorrs at a temperature above 1000°C. The furnace was filled with D_2 gas at a pressure of 30 lb in^{-2} (gauge) and the sample of palladium allowed to cool to room temperature. The degree of pre-loading was not measured directly, but similar experiments in a thermogravimetric balance suggested that we could achieve $[D]/[Pd] \approx 0.6$ by this strategy. The palladium cathode was positioned concentrically inside a 0.002 in platinum foil annular anode using PTFE spacers. The platinum anode was 5 cm long and 1.25 cm in inside diameter. The electrical connection to the anode was another 1.6 mm palladium lead sealed through the vessel lid with a PTFE Swagelok fitting.

Thermal calibration was accomplished by use of a heater (not shown) constructed with a 7–8 Ω resistive alloy wire wound onto an insulating form. Four copper leads were attached (for both current and potential measurements), and the heater assembly was immersed in silicone oil in a closed-ended glass tube of 6 mm outside diameter. Because we knew that the alkaline electrolyte would attack even quartz, the glass tube was inserted into a thin-walled platinum sheath which had been welded closed at its bottom end. This sheath was then sealed through the lid of the cell in a $\frac{1}{4}$ in PTFE Swagelok fitting.

The heat flow from this cell was measured by intercepting it externally to the brass can by a stream of water flowing in a 0.010 in annular space between the can

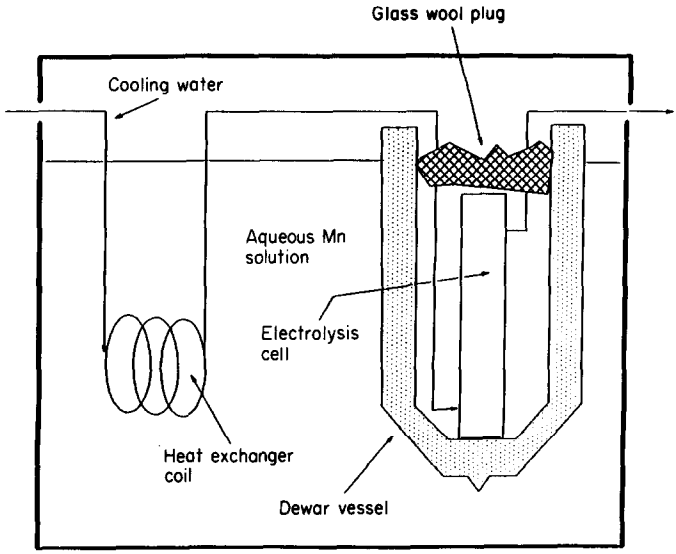

Fig. C2. Overall thermostatic environment for the closed cell.

and a PMMA jacket. The water flow was determined by the need to detect accurately the temperature difference between inlet and outlet. The flow, in the range of 5–15 ml min^{-1}, was adjusted according to the power dissipated in the cell. At these conditions, turbulence in the flowing water was negligible, and poor mixing was anticipated. We directed the water from the bottom to the top to avoid adverse free convection patterns. The temperature in the water was measured by calibrated thermistors arranged in a region of relatively high local convection at the entrance and exit to the cell cooling system. The readings were corroborated using calibrated platinum resistive thermometers. Finally, the cell was placed inside a Dewar vessel and wrapped with glass wool. The Dewar was held in a thermostatically controlled bath (Fig. C2), in which we circulated a concentrated aqueous solution of manganese nitrate (see eqn. (C4)).

Originally the water in the jacket was recirculated in a closed loop using a high performance liquid chromatography pump system; unfortunately, this proved unsatisfactory for the several weeks of the experiment because we experienced a number of mechanical failures. The pump eventually was replaced with a once-through water system using an overflow device to maintain the pressure head; the flow was measured several times a day by collecting the effluent in a graduated cylinder. Measured flows were constant to about ± 0.25 ml min^{-1}. The inlet temperature to the cell jacket was maintained by a copper coil heat exchanger immersed in the water bath.

Cell calibration

The wire-wound heater was used to calibrate the cell losses; these were a weak function of the cooling water rate and thermostatic bath temperature; so calibrations were run at a number of water rates, but we maintained a fixed water bath temperature to within about 0.3°C. In essence we measured the temperature rise of the water for a known dissipation in the calibrating heater. Typically the heat losses were about 10% of the input power. We did not systematically determine the source of this leak but simply added a correction factor to the calorimetrically determined heat evolved from the cell.

The measured heat flow Q_L to the water during calibration was proportional to the power P_{in} dissipated in the ohmic heater, i.e.

$$Q_L = kP_{in} \tag{C1}$$

where the proportionality constant $k = 0.097$ (at 9.0 ml min^{-1} flow rate) and 0.188 (at 5.0 ml min^{-1}).

Suppose that during a run under electrolysis conditions the measured heat flow to the flowing water is Q_{out} when the electric power is P_{in}. If excess heat Q_{ex} is generated in the cell, the energy balance reads

energy rate in = heat out

or

$$P_{in} + Q_{ex} = Q_{out} + k(P_{in} + Q_{ex}) \tag{C2}$$

since the heat losses must include a proportion of the imputed excess heat. Hence

$$1 + \frac{Q_{ex}}{P_{in}} = \frac{Q_{out}}{P_{in}(1-k)} \tag{C3}$$

All terms on the right-hand side of eqn. (C3) are measured quantities; this expression should sum to one ($\pm$experimental uncertainties) in the absence of any excess heat.

EXPERIMENTAL RESULTS

We filled the cell with 0.5 M LiOD in D_2O. By proton nuclear magnetic resonance measurement its protium content was about 0.05%. After 11 weeks this had risen to 1.5%, indicating some atmospheric leakage into the cell. We also measured the tritium content of (acidified) electrolyte using a standard scintillating cocktail as well as by looking unsuccessfully for increasing levels of 3 and 4 amu gases in vapor samples by mass spectrometry.

The cell was initially electrolyzed at a current density of about 100 mA cm^{-2} of cathode area. As a result of the rise in the pressure of O_2 in the cell, we calculated an uptake of deuterium of 0.69 [D]/[Pd] *additional to any absorbed during the*

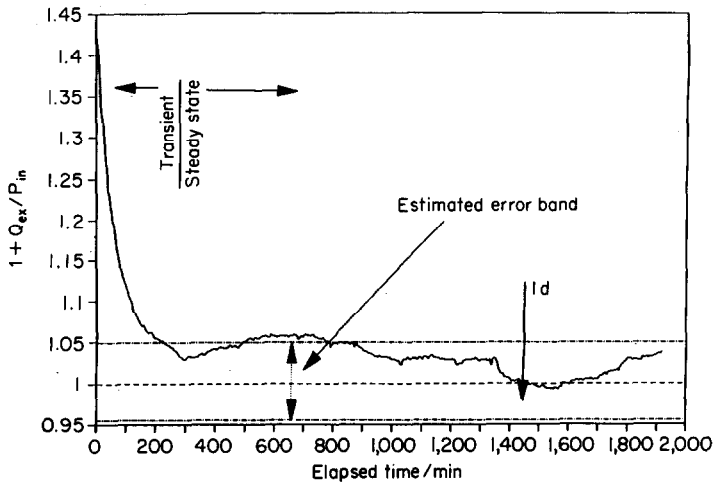

Fig. C3. Steady and unsteady heat flows from the closed cell.

palladium pre-loading procedure. Interestingly, about 90% of the uptake occurred in the first hour or so of electrolysis.

The manganese nitrate solution in the thermostatic bath was used to check for neutron production from the cell according to the nuclear reaction

$$n_0^1 + Mn^{55} \rightarrow Mn^{56}(t_{1/2} = 154 \text{ min}) + \gamma(0.847 \text{ MeV}) \qquad \text{(C4)}$$

The advantages of this reaction are that in this energy region the γ spectrum is relatively clear of naturally occurring spectral interferences, and a γ energy scan can be conducted remotely after the experiment but before the radiation decays. In addition, the cross-section of Mn^{55} to thermalized neutrons is very favorable compared with competing reactions. We used a 2×2 in NaI detector with a "Marinelli" liquid container to monitor samples of the manganese nitrate solution taken at regular intervals. No counts were seen in the spectral area of interest beyond what were expected from random background statistics.

The data were recorded on an analog-to-digital board and interpreted every few seconds to fit eqn. (C3). The derived left-hand side was plotted as a function of real time for many weeks. A typical early result is shown as Fig. C3. The transient shown in this figure is simply a manifestation of the heat capacity of the cell and its contents, and similar deviations of the ordinate from unity were observed when any power change (advertent or unintended) occurred. Other than such occasions, the ordinate stayed within the indicated $\pm 5\%$ error band. This error band was calculated by summing the uncertainties in the temperature difference in the water circuit and that due to uncertainties in the coolant flow rate. Of course, had Q_{ex} been greater than zero, the plotted function would have deviated from unity. The experiment ran for nearly 3 months, but the excess power curve was never significantly different from that shown in Fig. C3 except for inadvertent transients.

In summary, during electrolysis, we saw no evidence of excess heat, tritium, helium isotopes or neutron radiation at our levels of detection.